

The Solar-Type Contact Binary BX Pegasi Revisited

Jae Woo Lee, Seung-Lee Kim, Chung-Uk Lee, and Jae-Hyuck Youn

Korea Astronomy and Space Science Institute, Daejeon 305-348, Korea

`jwlee@kasi.re.kr, slkim@kasi.re.kr, leecu@kasi.re.kr, jhyoon@kasi.re.kr`

ABSTRACT

We present the results of new CCD photometry for the contact binary BX Peg, made during three successive months beginning on September 2008. As do historical light curves, our observations display an O’Connell effect and the November data by themselves indicate clear evidence for very short-time brightness disturbance. For these variations, model spots are applied separately to the two data set of Group I (Sep.–Oct.) and Group II (Nov.). The former is described by a single cool spot on the secondary photosphere and the latter by a two-spot model with a cool spot on the cool star and a hot one on either star. These are generalized manifestations of the magnetic activity of the binary system. Twenty light-curve timings calculated from Wilson-Devinney code were used for a period study, together with all other minimum epochs. The complex period changes of BX Peg can be sorted into a secular period decrease caused dominantly by angular momentum loss due to magnetic stellar wind braking, a light-travel-time (LTT) effect due to the orbit of a low-mass third companion, and a previously unknown short-term oscillation. This last period modulation could be produced either by a second LTT orbit with a period of about 16 yr due to the existence of a fourth body or by the effect of magnetic activity with a cycle length of about 12 yr.

Subject headings: Stars

1. INTRODUCTION

For BX Peg, Lee et al. (2004a, hereafter Lee04a) remains the most recent comprehensive study. These authors showed that historical light curves of BX Peg, displaying year-to-year light variability, can all be explained by introducing a single dark spot on the more massive secondary star and found that the orbital period has varied due to a periodic oscillation overlaid on a continuous period decrease. They concluded that the periodic $O-C$ residuals could not be produced by spot activity (Maceroni & van’t Veer 1994) and were not locked into the light variation as required by Applegate (1992). Thus, the only phenomenon that could be responsible was a third body with a period of 52.4 yr and a limiting mass of $M_3 \sin i_3 = 0.26 M_\odot$ and the hypothetical companion became the default explanation.

Lee04a also suggested that the timing residuals indicated an additional short-term oscillation with a period of about 12 yr and a semi-amplitude of about 0.002 d. Since then, many new photoelectric and CCD timings of minimum light have been reported and should now be sufficiently numerous to test this possibility meaningfully. In this article, we present a detailed study of the $O-C$ diagram of BX Peg together with a new light-curve synthesis.

2. NEW PHOTOMETRIC OBSERVATIONS

New CCD photometry of BX Peg was performed on 9 nights from 26 September through 15 November 2008. The observations were taken with a 2K CCD camera and a BVR filter set attached to the 1.0-m reflector at Mt. Lemmon Optical Astronomy Observatory (LOAO) in Arizona, USA. The instrument and reduction method have been described by Lee et al. (2009). The comparison star (C) was chosen to be BD + 25°4584 used in the previous observations by Zhai & Zhang (1979), Samec (1990), and Lee04a, all of whom reported no light variations for it. 2MASS 21392958+2637157 was selected as a check star (K) to verify the constancy in brightness of the comparison star. The reference stars were imaged on the CCD chip at the same time as the program star.

A total of 1,235 individual observations was obtained among the three bandpasses (411 in B , 412 in V , and 412 in R) and a sample of them is listed in Table 1. The light curves of BX Peg are plotted in the upper panel of Figure 1 and the (K–C) magnitude differences are shown in the lower panel. Measurements of the check star indicate that, on average, the comparison star remained constant within the 1σ -value of about ± 0.006 mag during our observing runs.

3. LIGHT-CURVE SYNTHESIS

Our light curves of BX Peg are asymmetrical and continue to display season-to-season light variability as they have in previous years. From the analysis of historical data, Lee04a showed that the asymmetries can be interpreted as spot activity on the secondary component presumably produced by a magnetic dynamo, and the variations of the asymmetries most likely arise from the variability of the spots with time. As shown in Figure 1, the new light curves still indicate an O’Connell effect (Max I fainter than Max II) and cycle-to-cycle intrinsic variability. Specifically, the November light curves are very different from the other data, especially at the first quadrature. We solved the new light curves in a manner almost identical to that used by Lee04a. For this synthesis, the contact mode 3 of the 2003 version¹ of the Wilson-Devinney code (Wilson & Devinney 1971; Wilson 1979, 1990; hereafter WD) was applied separately to the two data sets of Group I (Sep.–Oct.) and Group II (Nov.) and a cool spot on the secondary photosphere was adopted for both

¹<ftp://ftp.astro.ufl.edu/pub/wilson/>

Groups.

To start, we analyzed the light curves of Group I as reference ones. The photometric solutions are given in Table 2 and the spot parameters in the second column of Table 3, wherein the primary refers to the less massive hot star and the secondary to the more massive cool one. The results appear as the continuous curves in Figure 1 and the Group I and Group II residuals from this spot model are plotted in the left and middle panels of Figure 2, respectively. The single cool spot on the secondary represents the light curves of Group I satisfactorily, but a second spot is needed to explain the light residuals for Group II. Therefore, we modelled Group II data by adding a hot spot on the cool star and by adjusting only the spot and luminosity characteristics among the model parameters. These results are listed in columns (3)-(4) of Table 3 and the residuals from the model are plotted in the right panel of Figure 2, where we see that the hot spot is sufficient to explain the residual light discrepancy.

A separate trial, given in columns (5)-(6) of Table 3, testing for a hot spot on the primary star, was as successful as for the hot spot on the secondary so it is not possible to discriminate between these two possibilities. This troublesome degeneracy is due to the high inclination of the orbit and the radius difference between the stars causing such a hot spot to be visible throughout the same phase interval no matter to which star it is assigned. Lastly, we looked for a possible third light source (ℓ_3) but found that the code always returned negative values for this parameter.

In Lee04a it was shown that, within errors, 10 independent light curves obtained from 1978 through 2000 could all be represented by a unique geometry and by wavelength-consistent photometric parameters. That conclusion can now be extended to encompass the three 2008 light curves reported here. One must understand that the formal errors returned by the WD code are lower limits to realistic uncertainties but, even so, the agreement over 31 years is strong enough that the component stars of BX Peg are well known even within the formal errors. Perhaps this is not too surprising since the eclipses are complete and thus light curve determinacy is high, but the implication of the statement is that further photometric interest in this binary may be limited to mapping its intrinsic variability.

With this advantage, it is possible to ask whether there has been stability to the cool spots that have been described over the same time interval? Within assigned errors, these spots have migrated to larger longitudes over almost a hemisphere and (non-monotonically) have moved closer to the stellar equator. The spot sizes reached a maximum around 2000 and they have cooled progressively over the interval of monitoring. Of course, these conclusions depend on light curves that under-sample the time interval over which they were accumulated. It is also clear that a hot spot can emerge in a very brief time as happened over only a month in 2008. Almost certainly, this means that the hot spot is not a signature of impact from streaming gas since the over-contact condition has been documented since 1978. Rather, the hot disturbance and the variability of the cool spots are generalized manifestations of the magnetic activity of the BX Peg system.

4. FITTING THE $O-C$ VARIATION

We calculated minimum epochs for each of our eclipses with the WD code by means of adjusting only the ephemeris epoch (T_0). Ten such timings of minimum light are given in Table 4, together with all photoelectric and CCD timings since the compilation of Lee04a. For further ephemeris improvement, we used the light-curve timings given in Table 3 of Lee04a, rather than the original minima of Samec (1990). The following standard deviations were assigned to timing residuals based on observational technique and the method of measuring the epochs: ± 0.0036 d for visual and photographic, ± 0.0009 d for photoelectric and CCD, and ± 0.0003 d for WD minima. Relative weights were then scaled from the inverse squares of these values. Lee04a has shown that orbital period changes of BX Peg can be represented by a quadratic *plus* LTT ephemeris:

$$C_1 = T_0 + PE + AE^2 + \tau_3, \quad (1)$$

where τ_3 symbolizes the LTT due to a third companion physically bound to the eclipsing pair (Irwin 1952, 1959) and includes five parameters ($a_{12} \sin i_3$, e , ω , n and T). In order to improve the coefficients of the former ephemeris, we fitted all times of minimum light to equation (1) using the Levenberg-Marquart (LM) algorithm (Press et al. 1992). The results are given in the second column of Table 5, together with related parameters. The absolute dimensions of Samec & Hube (1991) have been used for these and subsequent calculations. The value for the third-companion period is different from the evaluation in Lee04a because the intervening years have added much weight to the period history. The other Irwin parameters have not changed significantly if one recognizes that ω is poorly determined even now.

The top panel of Figure 3 shows the $O-C_1$ residuals constructed with the linear term of the ephemeris; the solid curve and the dashed parabola represent the full non-linear terms and the quadratic term, respectively. The middle panel displays the residuals τ_3 from the linear and quadratic terms of the equation and the bottom panel the residuals from the complete ephemeris. These appear as $O-C_1$ in the third column of Table 4. In all panels, error bars are shown for only the timings with known errors. In the bottom panel of Figure 3, the timing residuals indicate, as before, a possible additional short-term oscillation. Accordingly, the period variability of the system must be more complicated than the form of equation (1). To get a more generalized description of the period variability, we introduced the times of minimum light into a different ephemeris form:

$$C_2 = T_0 + PE + AE^2 + \tau_3 + S, \quad S = K' \sin(\omega' E + \omega'_0). \quad (2)$$

The LM technique was again applied to solve for the eleven parameters of the ephemeris which are listed in the third column of Table 5. Adding the generalized sine modulation decreased the third-body period to a value close to that in Lee04a but nothing else has changed. The $O-C_2$ residuals from the linear light elements are plotted in the top panel of Figure 4. The second and third panels display the LTT orbit (τ_3) and a 12-yr period modulation (S), respectively, and the lowest panel the residuals from the full equation (2). These appear as $O-C_2$ in the fourth column of Table 4. It is clear that the residuals in the third panel of Figure 4 skew across the sine curve

and the fit is not so good as could be wished. Consequently, the lowest panel of the figure does not show the final residuals as randomized as they should be.

The sine oscillation can be replaced in favor of a second LTT orbit ascribed to a fourth component of the BX Peg system. For such a case, it is necessary to use a quadratic *plus* two-LTT ephemeris instead of equation (2):

$$C_3 = T_0 + PE + AE^2 + \tau_3 + \tau_4. \quad (3)$$

These calculations converged quickly to yield the entries listed in Table 6 where we see that not much has changed for the orbit of the supposed third object of the system. Figure 5, derived from the Table 6 parameters, is plotted in the same sense as Figure 4. The second and third panels refer to the τ_3 and τ_4 orbits, respectively, and are possibly marginally better fits to the data. If the hypothetical objects are on the main sequence, the minimum masses for the putative third and fourth bodies correspond to spectral types of M6 and M8, respectively, and their bolometric luminosities would contribute only 0.6 % to the total luminosity of the quadruple system. Also, the semi-amplitude of the systemic radial velocity variation of the eclipsing pair due to the two supposed companions would be only about 1 km s⁻¹. These two limits indicate that it will be not easy to detect companions orbiting the eclipsing binary independently.

As predicted by Maceroni & van't Veer (1994) and confirmed by Lee et al. (2009), times of minimum light may be systematically shifted by light asymmetries due to starspot activity. The light curve synthesis method gives more precise timings than do other techniques (e.g. Kwee & van Woerden 1956) based on the observations during a minimum alone. Clear evidence for this assertion appears in Figures 3–5 which show almost no noise for the WD timings compared to those from other methods.

5. DISCUSSION

The negative coefficients of the quadratic terms in equations (2) and (3) yield a continuous period decrease with a rate of -9.8×10^{-8} d yr⁻¹, which can be explained either by conservative mass transfer from the more massive cool star to its less massive hot component or by angular momentum loss (AML) due to a magnetic stellar wind. Under the assumption of conservative mass transfer, the transfer rate is about $7.0 \times 10^{-8} M_{\odot}$ yr⁻¹. This value is 3.5 times greater than a rate of $2.0 \times 10^{-8} M_{\odot}$ yr⁻¹ calculated by assuming that the cool secondary transfers mass to the hot primary component on a thermal time scale. Therefore, the alternative mechanism, AML caused by magnetic braking rooted in the convective zone, seems more likely. From an approximate formula given by Guinan & Bradstreet (1988), the period decrease rate is calculated to -4.1 , -5.8 , and -8.7 (in units of 10^{-8} d yr⁻¹) for $k^2=0.07$, 0.10, and 0.15, respectively. The last value might be a good approximation to the gyration constant k^2 of BX Peg. It is also possible that the correct explanation of the secular period change is some combination of non-conservative mass transfer and AML but, at present, it seems that AML should be the dominant contributor.

This last cautionary remark actually has some independent support. Consider the pair of W-type systems defined observationally by Binnendijk (1970), V829 Her (Erdem & Özkardeş 2006) and V781 Tau (Yakut et al. 2005). Their individual masses and radii and the photospheric temperature difference as well as the systemic mass ratio and period are the same values within 1 % yet the algebraic signs of the secular period changes are different. This is not a unique case. The same situation exists for V417 Aql (Qian 2003; Lee et al. 2004b) and BB Peg (Kalomeni et al. 2007). If there is little mechanical and radiometric difference between two such binaries which behave differently dynamically, there must be a particular evolutionary mechanism that distinguishes them or else the seeming secular period changes are not really unbounded and are just long-term cyclical effects. The rigorous association of a positive period change with a particular sense of mass transfer and the mirror association of a negative period change with the other sense of mass transfer and with AML appear to be too didactic.

The 12-yr period modulation, shown in the third panel of Figure 4, could operate in at least one component since each has a convective envelope and thus may be magnetically active (Applegate 1992; Lanza et al. 1998). With the values of K' and P' , the parameters of an Applegate model were calculated for both components and appear in Table 7, where Δm_{rms} denotes a bolometric magnitude difference relative to the mean light level of BX Peg converted to magnitude scale with equation (4) in the paper of Kim et al. (1997). The variations of the gravitational quadrupole moment ΔQ correspond to typical values for contact binaries and the required light variation associated with each component is within the value ($\Delta L/L_{p,s} \sim 0.1$) proposed by Applegate. This consistency indicates that Applegate’s mechanism could possibly function in both component stars. There is no *a priori* reason to require a sine-type behavior for a magnetic cycle in a star. If Applegate’s mechanism is the main cause of the cyclical variation, his model requires the brightness variation to vary in phase with the period modulation of Figure 4.

In order to check this possibility and to study the long-term light variations of BX Peg, we measured the light levels at four different phases (Max I, Min I, Max II and Min II) for our new light curves and for the archival measurements of Zhai & Zhang (1979), Samec (1990) and Lee04a. The latter are taken from Table 6 of Lee04a and the comparisons are given in Table 8. All data sets are referred to the same comparison star (BD + 25°4584). The brightness variations of ΔB and ΔV are plotted in Figure 6, where the seasonal means were subtracted from the grand mean for all seasons giving the mean seasonal differences in the natural systems. The year and epoch for each data set were calculated by averaging the starting and ending HJDs of the observations. In Figure 6, the third and fourth panels represent the sine term of the C_2 ephemeris and the τ_4 orbit of the C_3 ephemeris, respectively, averaged over each observing season and the arrows indicate the mean epoch of each seasonal light curve. There are only 5 epochs for light curves but, even as few as they are, they do not conform to this prediction of the Applegate mechanism.

This binary presents a conflict for observers. Without the minimum monitoring which has been so fruitful, we would be ignorant of the time-scales and semi-amplitudes of the 50-year cycle and of the shorter one as well. Perusal of the present Figures 3 through 5 and of Figures 4 and 5

in Lee04a shows that the 50-year cycle has become much better delineated over only 5 years. The same conclusion cannot be drawn for the shorter cycle. We have already remarked that neither the sinusoid nor a fourth-companion waveform track the residuals well. Many of the minimum timings are much less precise than those from LOAO and their noisy appearance is readily evident in all the figures. Residuals as large as -3.7 minutes appear in Table 4, a value that is almost 1 % of the Keplerian period and more than 4 % of the entire eclipse width. Such discrepancies probably do not signify high-frequency spot activity; at least there is no independent evidence for such a possibility. Rather, they must be the result of clerical or observational errors or of greatly-undersampled timing determinations.

The authors wish to thank Dr. Robert H. Koch for careful readings and corrections and for some helpful comments on the draft version of the manuscript. We also thank the staff of Mt. Lemmon Optical Astronomy Observatory for assistance with our observations. This research has made use of the Simbad database maintained at CDS, Strasbourg, France.

REFERENCES

- Applegate, J. H. 1992, *ApJ*, 385, 621
- Binnendijk, L. 1970, *Vistas Astron.*, 12, 217
- Brát, L., Zejda, M., & Svoboda, P. 2007, *Open Eur. J. Var. Stars*, 74, 1
- Diethelm, R. 2004, *Inf. Bull. Var. Stars*, No. 5543
- Diethelm, R. 2005, *Inf. Bull. Var. Stars*, No. 5653
- Doğru, S. S., Dönmez, A., Tüysüz, M., Doğru, D., Özkardeş, B., Soydugan, E., & Soydugan, F. 2007, *Inf. Bull. Var. Stars*, No. 5746
- Erdem, A., & Özkardeş, B. 2006, *New Astron.*, 12, 192
- Guinan, E. F., & Bradstreet, D. H. 1988, in *Formation and Evolution of Low Mass Stars*, eds. A. K. Dupree and M. T. V. T. Lago (Dordrecht: Kluwer), 345
- Hübscher, J. 2005, *Inf. Bull. Var. Stars*, No. 5643
- Hübscher, J., Paschke, A., & Walter, F. 2005, *Inf. Bull. Var. Stars*, No. 5657
- Hübscher, J., Paschke, A., & Walter, F. 2006, *Inf. Bull. Var. Stars*, No. 5731
- Hübscher, J., & Walter, F. 2007, *Inf. Bull. Var. Stars*, No. 5761
- Irwin, J. B. 1952, *ApJ*, 116, 211
- Irwin, J. B. 1959, *AJ*, 64, 149
- Kalomeni, B., Yakut, K., Keskin, V., Değirmenci, Ö. L., Ulaş, B., & Köse, O. 2007, *AJ*, 134, 642
- Kim, C.-H., Jeong, J. H., Demircan, O., Müyesseroğlu, Z., & Budding, E. 1997, *AJ*, 114, 2753
- Krajci, T. 2005, *Inf. Bull. Var. Stars*, No. 5592
- Kwee, K. K., & van Woerden, H. 1956, *Bull. Astron. Inst. Neth.*, 12, 327
- Lanza, A. F., Rodono, M., & Rosner, R. 1998, *MNRAS*, 296, 893
- Lee, J. W., Kim, C.-H., Han, W., Kim, H.-I., & Koch, R. H. 2004a, *MNRAS*, 352, 1041 (Lee04a)
- Lee, J. W., Kim, C.-H., Lee, C.-U., & Oh, K.-D. 2004b, *J. Astron. Space Sci.*, 21, 73
- Lee, J. W., Youn, J.-H., Lee, C.-U., Kim, S.-L., & Koch, R. H. 2009, *AJ*, 138, 478
- Maceroni, C., & van't Veer, F. 1994, *A&A*, 289, 871

- Nagai, K. 2006, VSOLJ Var. Star Bull., 44, 7
- Nagai, K. 2007, VSOLJ Var. Star Bull., 45, 6
- Nagai, K. 2008, VSOLJ Var. Star Bull., 46, 5
- Ogloza, W., Niewiadomski, W., Barnacka, A., Biskup, M., Malek, K., & Sokolowski, M. 2008, Inf. Bull. Var. Stars, No. 5843
- Paschke, A. 2007, Open Eur. J. Var. Stars, 73, 1
- Press, W. H., Teukolsky, S. A., Vetterling, W. T., & Flannery, B. P. 1992, Numerical Recipes (Cambridge: Cambridge Univ. Press), Chapter 15
- Pribulla, T., et al. 2005, Inf. Bull. Var. Stars, No. 5668
- Qian, S. 2003, A&A, 400, 649
- Samec, R. G. 1990, AJ, 100, 808
- Samec, R. G., & Hube, D. P. 1991, AJ, 102, 1171
- Samolyk, G. 2008a, J.AAVSO, 36, 171
- Samolyk, G. 2008b, J.AAVSO, 36, 186
- Wilson, R. E. 1979, ApJ, 234, 1054
- Wilson, R. E. 1990, ApJ, 356, 613
- Wilson, R. E., & Devinney, E. J. 1971, ApJ, 166, 605
- Yakut, K., Ulaş, B., Kalomeni, B., & Gülmen, Ö. 2005, MNRAS, 363, 1272
- Zejda, M. 2004, Inf. Bull. Var. Stars, No. 5583
- Zejda, M., Mikulášek, Z., & Wolf, M. 2006, Inf. Bull. Var. Stars, No. 5741
- Zhai, D., & Zhang, Y. 1979, Xexue Tongbao, 21, 986

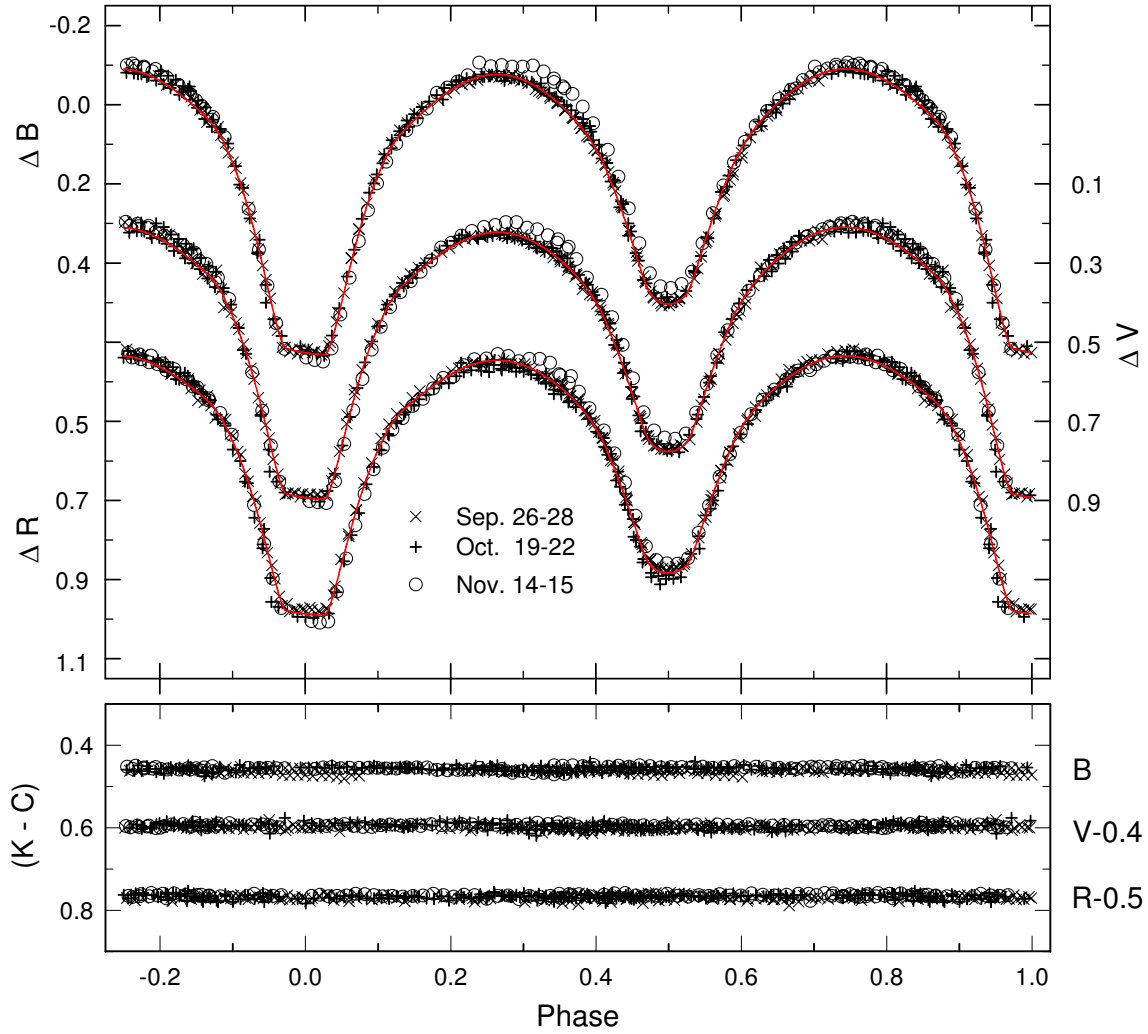


Fig. 1.— The upper panel displays BVR light curves of BX Peg defined by individual observations. The solid curves represent the photometric solutions obtained from the measurements between September and October 2008. The magnitude differences $(K-C)$ between the check and comparison stars are plotted in the lower panel.

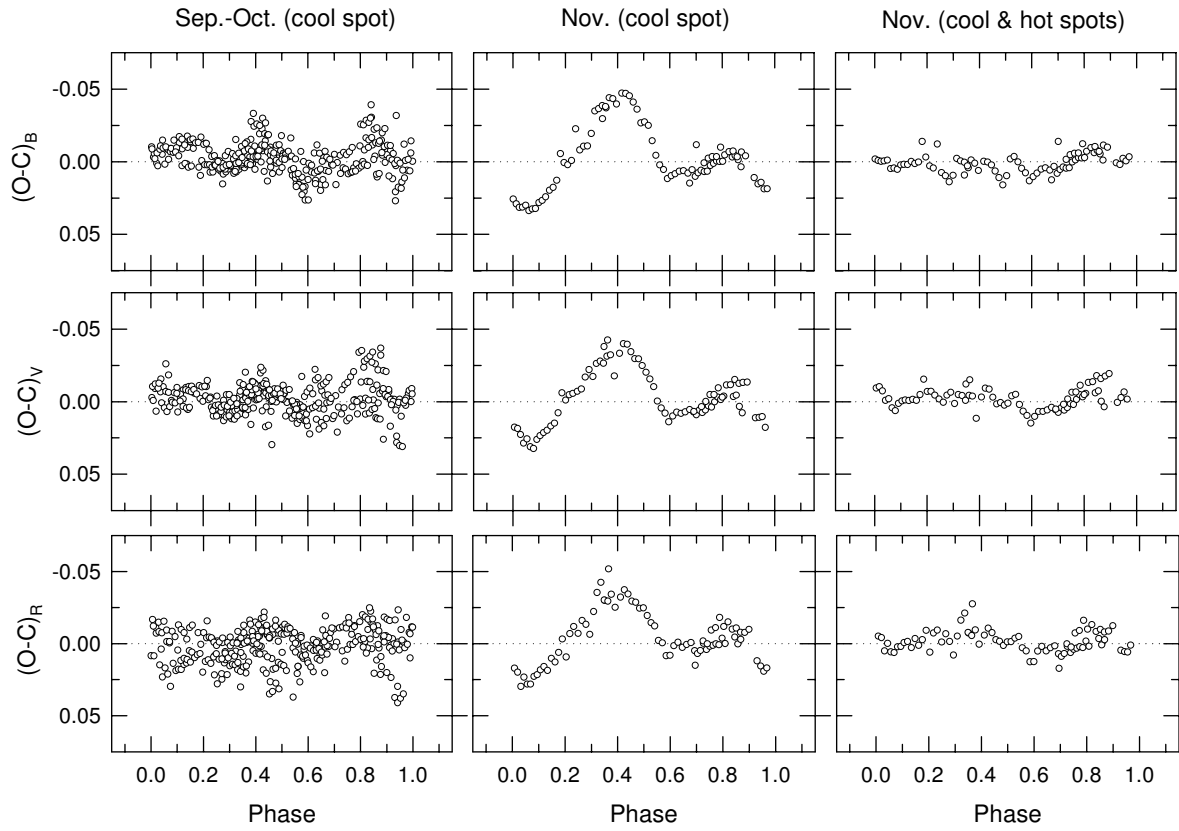


Fig. 2.— Light residuals from the models for two data sets (Group I and Group II). See the text for details.

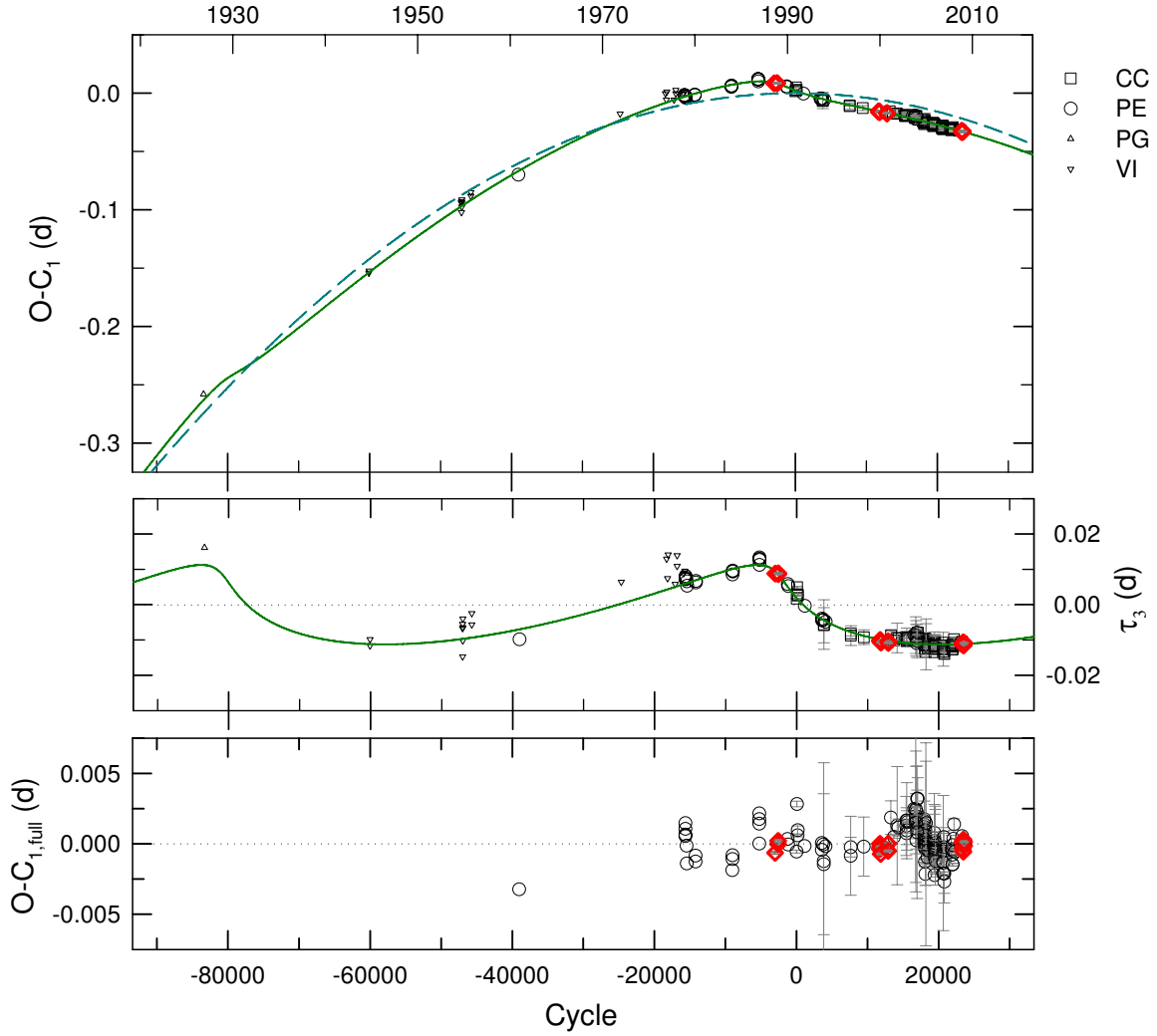


Fig. 3.— The $O-C_1$ diagram of BX Peg constructed with the linear terms of the quadratic *plus* LTT ephemeris. In the top panel, the continuous curve and the dashed, parabolic one represent the full contribution and the quadratic term of the equation, respectively. Diamond symbols refer to the minimum times obtained with the WD code. The middle panel displays the residuals from the linear and quadratic terms and the bottom panel the residuals from the full ephemeris. An additional short-term oscillation seems to exist in the final residuals in the bottom panel.

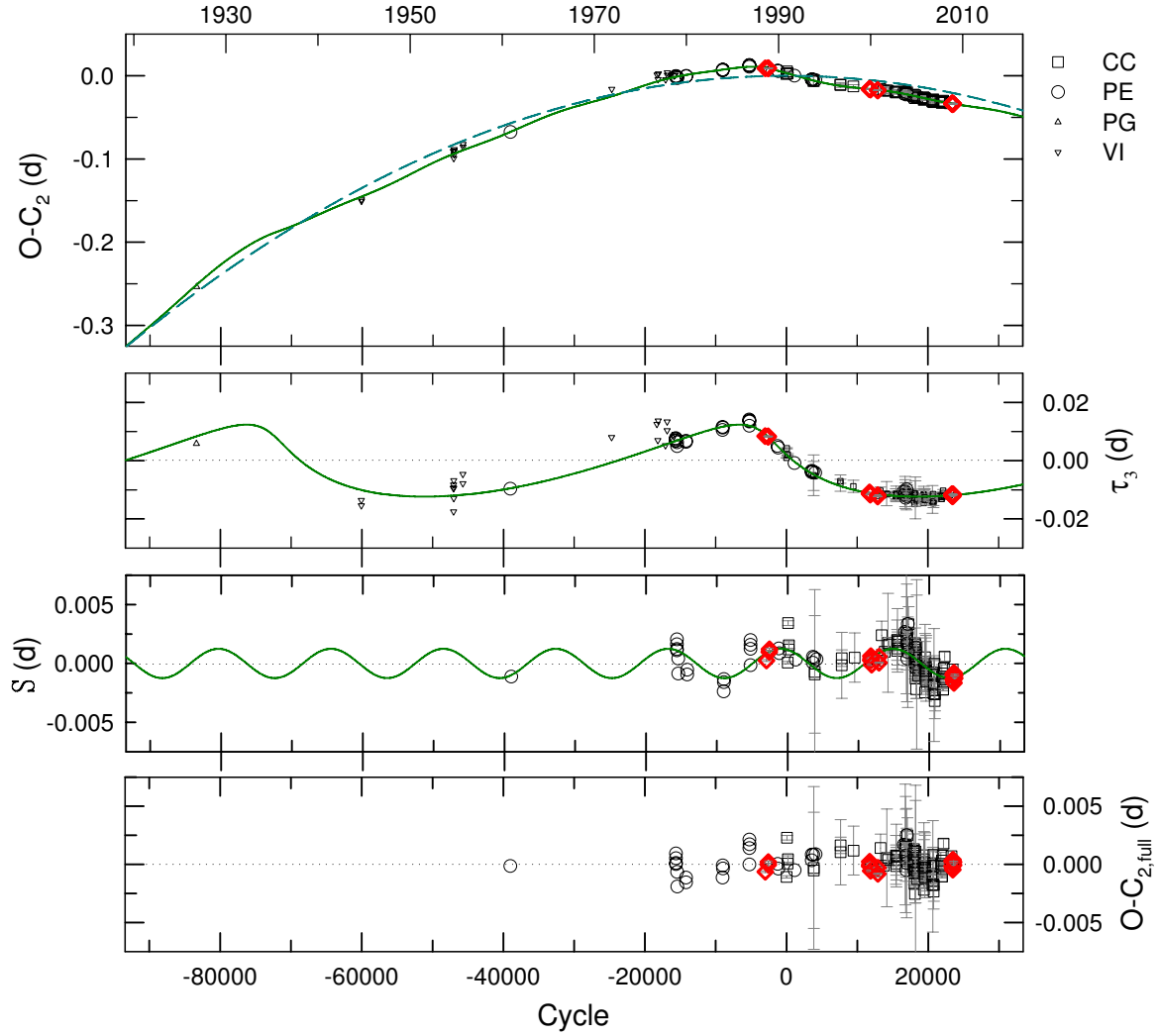


Fig. 4.— The $O-C_2$ residuals of BX Peg from the linear ephemeris of equation (2). These are drawn in the top panel with the continuous curves due to the full non-linear terms and the dashed parabola due to the quadratic term of the equation. The second and third panels display a LTT orbit and a 12-yr period oscillation, respectively, and the lowest panel the residuals from the complete equation.

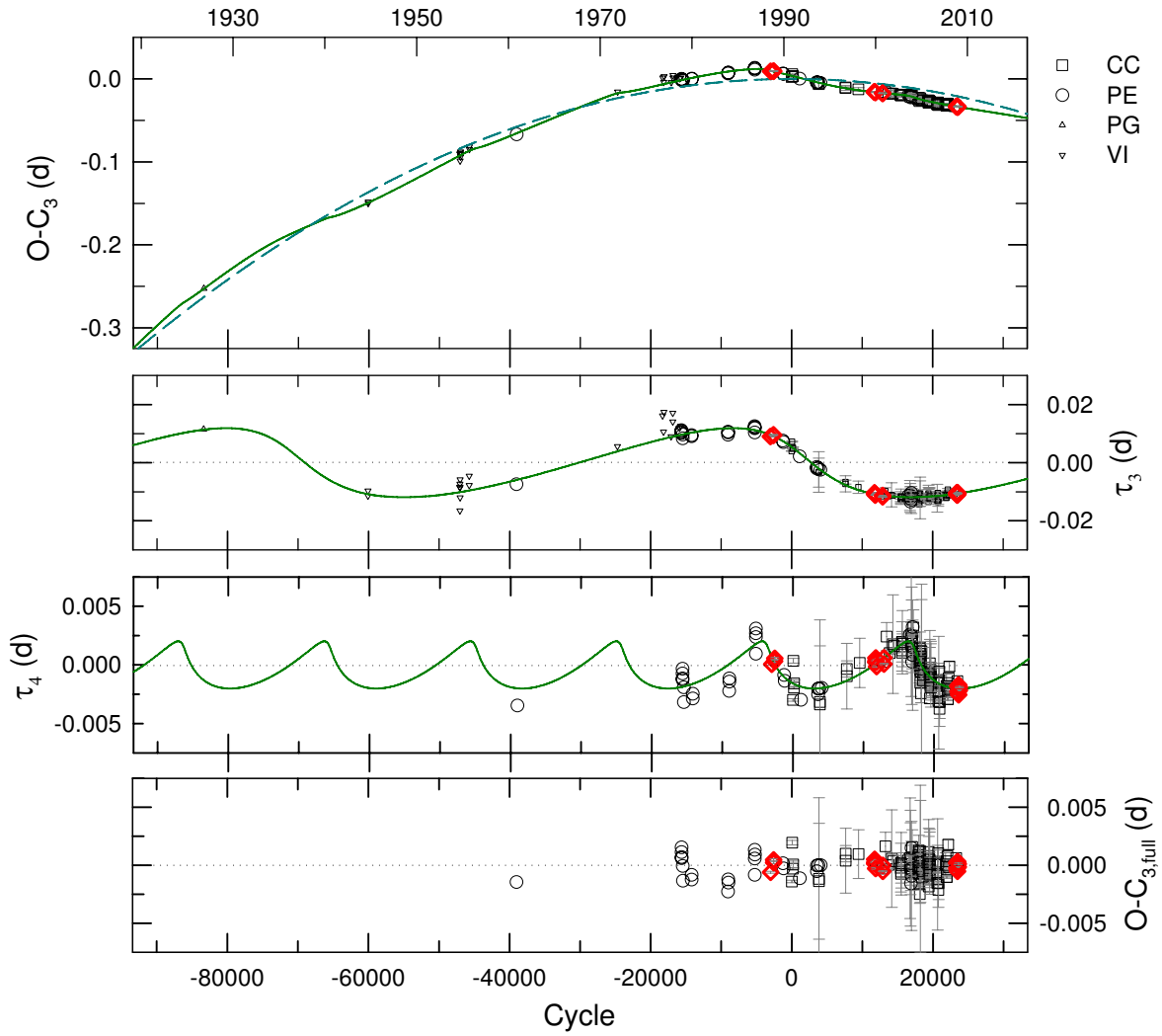


Fig. 5.— The upper panel is constructed in the same sense as Figure 4 with the linear terms of Table 6. The second and third panels refer to the τ_3 and τ_4 orbits, respectively.

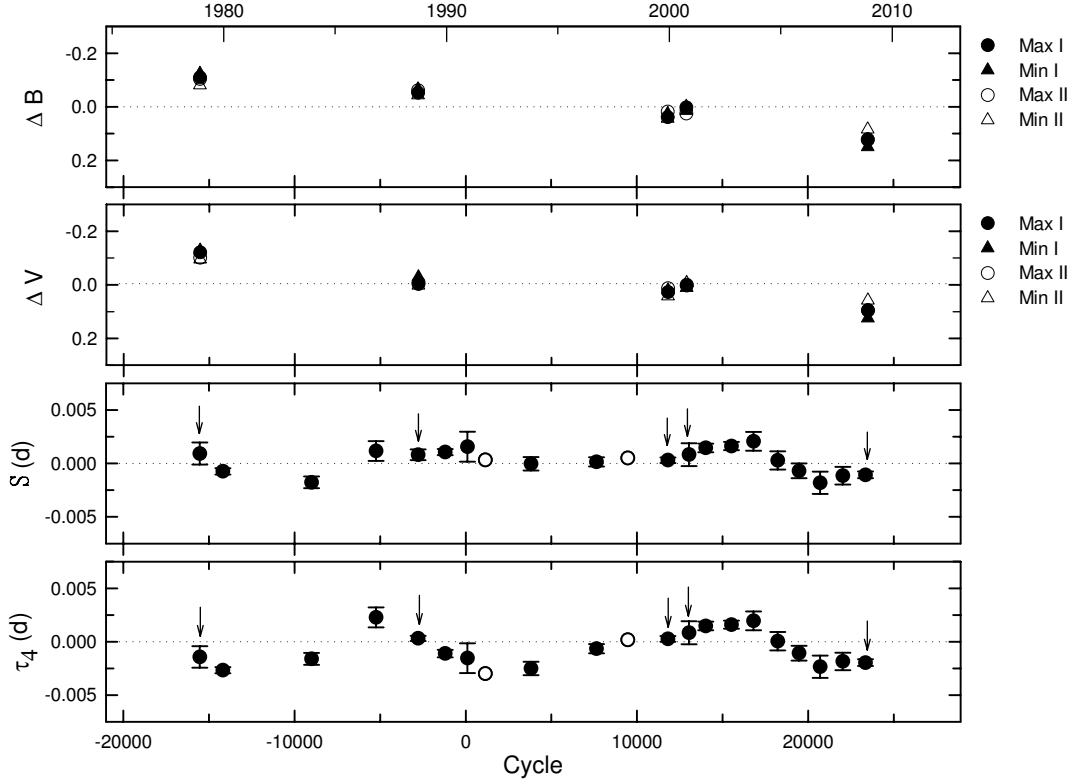


Fig. 6.— The mean seasonal variations of ΔB and ΔV for BX Peg at four characteristic phases (Max I, Min I, Max II and Min II). The third and fourth panels represent the sine term and the τ_3 orbit of the C_2 and C_3 ephemeris forms, respectively, averaged over each observing season and the plotted points were determined by combining all eclipse timings for a given year. Open circles refer to seasons with only one minimum timing. An errors bar gives the standard deviation of each data set. The arrows indicate the mean epoch of each seasonal light curve.

Table 1. CCD photometric observations of BX Peg.

HJD	ΔB	HJD	ΔV	HJD	ΔR
2,454,736.66243	−0.070	2,454,736.66347	0.227	2,454,736.66423	0.346
2,454,736.66521	−0.066	2,454,736.66625	0.231	2,454,736.66701	0.355
2,454,736.66800	−0.064	2,454,736.66904	0.235	2,454,736.66978	0.353
2,454,736.67080	−0.060	2,454,736.67190	0.242	2,454,736.67265	0.362
2,454,736.67367	−0.054	2,454,736.67477	0.250	2,454,736.67549	0.368
2,454,736.67652	−0.039	2,454,736.67761	0.259	2,454,736.67835	0.384
2,454,736.67938	−0.028	2,454,736.68047	0.270	2,454,736.68120	0.388
2,454,736.68221	−0.016	2,454,736.68331	0.286	2,454,736.68404	0.404
2,454,736.68505	−0.003	2,454,736.68614	0.297	2,454,736.68687	0.417
2,454,736.68788	0.015	2,454,736.68898	0.318	2,454,736.68972	0.430

Note. — This table is available in its entirety in machine-readable and Virtual Observatory (VO) forms in the online journal. A portion is shown here for guidance regarding its form and content.

Table 2. Photometric solutions of BX Peg.

Parameter	Primary	Secondary
T_0 (HJD)	2,453,208.3118±0.0035	
P (d)	0.28041759±0.00000064	
q	2.6897±0.0045	
i (deg)	87.693±0.095	
T (K)	5532±20	5300
Ω	6.135±0.010	6.135
A	0.5	0.5
g	0.32	0.32
X	0.517	0.525
x_B	0.636±0.049	0.662±0.018
x_V	0.440±0.044	0.591±0.017
x_R	0.334±0.040	0.516±0.018
$L/(L_1 + L_2)_B$	0.352±0.001	0.648
$L/(L_1 + L_2)_V$	0.348±0.001	0.652
$L/(L_1 + L_2)_R$	0.341±0.001	0.659
r (pole)	0.2820±0.0009	0.4435±0.0007
r (side)	0.2946±0.0010	0.4752±0.0009
r (back)	0.3310±0.0016	0.5034±0.0012
r (volume) ^a	0.3042	0.4755

^aMean volume radius.

Table 3. Spot parameters for BX Peg.^a

Parameter	Group I	Group II			
	Cool 2	Cool 2 and Hot 2		Cool 2 and Hot 1	
Colatitude (deg)	66.6±2.1	76.2±1.5	61.5±1.4	78.7±0.6	68.3±3.2
Longitude (deg)	142.7±0.4	143.7±2.0	40.7±3.1	140.2±0.3	230.0±1.1
Radius (deg)	14.1±0.1	15.1±1.2	14.6±2.0	15.7±0.1	20.7±0.8
$T_{\text{spot}}/T_{\text{local}}$	0.828±0.050	0.751±0.031	1.122±0.005	0.762±0.025	1.117±0.011

^aCool 2: a cool spot on the secondary; Hot 2: a hot spot on the secondary; Hot 1: a hot spot on the primary.

Table 4. Observed photoelectric and CCD times of minimum light for BX Peg since the compilation of Lee04a.

HJD (2,450,000+)	Epoch	$O-C_1$	$O-C_2$	$O-C_3$	Min	References
1,899.3225	13283.0	0.00186	0.00140	0.00164	I	Brát et al. (2007)
2,145.5289	14161.0	0.00129	0.00056	0.00057	I	Zejda (2004)
2,521.4288	15501.5	0.00095	0.00006	-0.00056	II	Zejda (2004)
2,521.5697	15502.0	0.00164	0.00075	0.00013	I	Zejda (2004)
2,878.4018	16774.5	0.00197	0.00122	0.00012	II	Hübscher et al. (2005)
2,878.5425	16775.0	0.00246	0.00171	0.00061	I	Hübscher et al. (2005)
2,886.3935	16803.0	0.00176	0.00102	-0.00008	I	Krajci (2005)
2,887.3756	16806.5	0.00240	0.00165	0.00056	II	Hübscher (2005)
2,887.5149	16807.0	0.00149	0.00074	-0.00035	I	Hübscher (2005)
2,887.515	16807.0	0.00159	0.00084	-0.00025	I	Diethelm (2004)
2,902.3758	16860.0	0.00024	-0.00049	-0.00157	I	Hübscher (2005)
2,929.4367	16956.5	0.00082	0.00011	-0.00092	II	Hübscher (2005)
2,929.5793	16957.0	0.00321	0.00250	0.00147	I	Hübscher (2005)
2,956.3592	17052.5	0.00320	0.00251	0.00156	II	Brát et al. (2007)
3,208.4530	17951.5	0.00137	0.00092	0.00086	II	Pribulla et al. (2005)
3,209.4332	17955.0	0.00010	-0.00034	-0.00040	I	Hübscher et al. (2005)
3,209.4335	17955.0	0.00040	-0.00004	-0.00010	I	Pribulla et al. (2005)
3,209.5743	17955.5	0.00099	0.00055	0.00049	II	Pribulla et al. (2005)
3,212.5180	17966.0	0.00031	-0.00013	-0.00018	I	Pribulla et al. (2005)
3,217.4262	17983.5	0.00120	0.00076	0.00072	II	Hübscher et al. (2005)
3,220.3701	17994.0	0.00071	0.00028	0.00025	I	Pribulla et al. (2005)
3,220.5099	17994.5	0.00030	-0.00013	-0.00016	II	Pribulla et al. (2005)
3,220.5112	17994.5	0.00160	0.00117	0.00114	II	Hübscher et al. (2005)
3,221.4928	17998.0	0.00174	0.00131	0.00128	I	Hübscher et al. (2005)
3,224.4358	18008.5	0.00035	-0.00008	-0.00010	II	Pribulla et al. (2005)
3,226.5392	18016.0	0.00062	0.00019	0.00018	I	Pribulla et al. (2005)
3,226.5392	18016.0	0.00062	0.00019	0.00018	I	Hübscher et al. (2005)
3,228.3612	18022.5	-0.00010	-0.00052	-0.00053	II	Brát et al. (2007)
3,233.4095	18040.5	0.00068	0.00026	0.00026	II	Hübscher et al. (2005)
3,233.5488	18041.0	-0.00023	-0.00065	-0.00065	I	Hübscher et al. (2005)
3,236.3538	18051.0	0.00059	0.00018	0.00019	I	Pribulla et al. (2005)
3,236.4931	18051.5	-0.00032	-0.00073	-0.00072	II	Pribulla et al. (2005)
3,240.4180	18065.5	-0.00127	-0.00168	-0.00166	II	Pribulla et al. (2005)
3,240.5597	18066.0	0.00023	-0.00019	-0.00017	I	Pribulla et al. (2005)
3,250.3747	18101.0	0.00060	0.00020	0.00024	I	Hübscher et al. (2005)
3,250.5140	18101.5	-0.00031	-0.00071	-0.00067	II	Hübscher et al. (2005)
3,255.4219	18119.0	0.00028	-0.00011	-0.00006	I	Hübscher et al. (2005)
3,255.5628	18119.5	0.00097	0.00058	0.00063	II	Hübscher et al. (2005)
3,257.3845	18126.0	-0.00004	-0.00044	-0.00038	I	Hübscher et al. (2005)
3,257.5226	18126.5	-0.00215	-0.00254	-0.00249	II	Hübscher et al. (2005)
3,282.3417	18215.0	-0.00003	-0.00039	-0.00029	I	Hübscher et al. (2005)
3,282.4834	18215.5	0.00146	0.00110	0.00120	II	Hübscher et al. (2005)
3,341.2285	18425.0	-0.00097	-0.00126	-0.00106	I	Diethelm (2005)
3,360.2974	18493.0	-0.00048	-0.00075	-0.00053	I	Zejda et al. (2006)
3,601.4569	19353.0	-0.00027	-0.00027	0.00010	I	Hübscher et al. (2006)

Table 4—Continued

HJD (2,450,000+)	Epoch	$O-C_1$	$O-C_2$	$O-C_3$	Min	References
3,613.3741	19395.5	-0.00083	-0.00081	-0.00044	II	Hübscher et al. (2006)
3,613.5150	19396.0	-0.00013	-0.00012	0.00025	I	Zejda et al. (2006)
3,613.5159	19396.0	0.00077	0.00078	0.00115	I	Hübscher et al. (2006)
3,614.3566	19399.0	0.00021	0.00023	0.00059	I	Brát et al. (2007)
3,614.4970	19399.5	0.00040	0.00042	0.00079	II	Hübscher et al. (2006)
3,616.4573	19406.5	-0.00222	-0.00220	-0.00184	II	Brát et al. (2007)
3,617.4407	19410.0	-0.00028	-0.00026	0.00010	I	Brát et al. (2007)
3,632.0216	19462.0	-0.00111	-0.00107	-0.00071	I	Nagai (2006)
3,632.1623	19462.5	-0.00062	-0.00058	-0.00021	II	Nagai (2006)
3,648.4272	19520.5	0.00005	0.00011	0.00047	II	Hübscher et al. (2006)
3,651.3711	19531.0	-0.00043	-0.00038	-0.00001	I	Brát et al. (2007)
3,651.3714	19531.0	-0.00013	-0.00008	0.00029	I	Hübscher et al. (2006)
3,651.5111	19531.5	-0.00064	-0.00059	-0.00022	II	Hübscher et al. (2006)
3,659.3629	19559.5	-0.00054	-0.00047	-0.00011	II	Hübscher et al. (2006)
3,659.5033	19560.0	-0.00035	-0.00028	0.00008	I	Hübscher et al. (2006)
3,663.9891	19576.0	-0.00123	-0.00116	-0.00080	I	Nagai (2006)
3,951.1360	20600.0	-0.00209	-0.00177	-0.00152	I	Nagai (2007)
3,951.2770	20600.5	-0.00129	-0.00098	-0.00073	II	Nagai (2007)
3,966.4203	20654.5	-0.00055	-0.00022	0.00002	II	Hübscher & Walter (2007)
3,966.5597	20655.0	-0.00136	-0.00103	-0.00079	I	Hübscher & Walter (2007)
3,985.4890	20722.5	-0.00025	0.00009	0.00031	II	Doğru et al. (2007)
3,989.6960	20737.5	0.00048	0.00082	0.00105	II	Ogloza et al. (2008)
3,992.3574	20747.0	-0.00209	-0.00174	-0.00152	I	Hübscher & Walter (2007)
4,000.3487	20775.5	-0.00269	-0.00234	-0.00213	II	Brát et al. (2007)
4,002.4524	20783.0	-0.00212	-0.00178	-0.00156	I	Hübscher & Walter (2007)
4,279.647	21771.5	-0.00040	0.00003	0.00008	II	Paschke (2007)
4,327.4581	21942.0	-0.00050	-0.00008	-0.00006	I	Brát et al. (2007)
4,328.4386	21945.5	-0.00147	-0.00105	-0.00102	II	Brát et al. (2007)
4,328.4386	21945.5	-0.00147	-0.00105	-0.00102	II	Brát et al. (2007)
4,328.4393	21945.5	-0.00077	-0.00035	-0.00032	II	Brát et al. (2007)
4,330.5428	21953.0	-0.00040	0.00002	0.00004	I	Brát et al. (2007)
4,330.5431	21953.0	-0.00010	0.00032	0.00034	I	Brát et al. (2007)
4,359.9874	22058.0	0.00035	0.00076	0.00077	I	Nagai (2008)
4,386.6281	22153.0	0.00138	0.00178	0.00178	I	Samolyk (2008a)
4,420.5567	22274.0	-0.00056	-0.00017	-0.00018	I	Samolyk (2008a)
4,650.7799	23095.0	-0.00021	0.00002	-0.00006	I	Samolyk (2008b)
4,702.6579	23280.0	0.00054	0.00071	0.00062	I	Samolyk (2008b)
4,736.72819	23401.5	0.00009	0.00022	0.00014	II	this article
4,736.86805	23402.0	-0.00026	-0.00012	-0.00021	I	this article
4,737.70921	23405.0	-0.00035	-0.00022	-0.00031	I	this article
4,737.84996	23405.5	0.00019	0.00032	0.00024	II	this article
4,738.69117	23408.5	0.00015	0.00028	0.00019	II	this article
4,759.72254	23483.5	0.00020	0.00030	0.00022	II	this article
4,760.70325	23487.0	-0.00055	-0.00045	-0.00053	I	this article
4,761.68556	23490.5	0.00030	0.00040	0.00031	II	this article

Table 4—Continued

HJD (2,450,000+)	Epoch	$O-C_1$	$O-C_2$	$O-C_3$	Min	References
4,785.66083	23576.0	-0.00013	-0.00006	-0.00015	I	this article
4,786.64256	23579.5	0.00014	0.00020	0.00012	II	this article

Table 5. The fitting parameters for ephemeris forms (1) and (2) for BX Peg.^a

Parameter	Equation (1)	Equation (2)	Unit
T_0	2,448,174.52857(31)	2,448,174.52814(23)	HJD
P	0.280419296(18)	0.280419347(13)	d
$a_{12} \sin i_3$	2.464(75)	2.458(50)	AU
ω	148.9(3.0)	141.4(2.1)	deg
e	0.715(36)	0.627(38)	
n	0.016535(92)	0.018422(73)	deg d ⁻¹
T	2,425,845(123)	2,427,824(80)	HJD
P_3	59.61(33)	53.50(21)	yr
K	0.01126(34)	0.01238(25)	d
$f(M_3)$	0.00421(13)	0.00519(11)	M_\odot
$M_3 \sin i_3$	0.223(4)	0.241(2)	M_\odot
A	$-3.944(77) \times 10^{-11}$	$-3.736(56) \times 10^{-11}$	d
dP/dt	$-10.28(20) \times 10^{-8}$	$-9.73(15) \times 10^{-8}$	d yr ⁻¹
K'	...	0.00124(31)	d
ω'	...	0.0227(10)	deg P^{-1}
ω'_0	...	112(16)	deg
P'	...	12.2(1.9)	yr

^aA parenthesized number is the 1σ -value of the last two digits of each parameter.

Table 6. Parameters for the quadratic *plus* two-LTT ephemeris of BX Peg.

Parameter	Third body	Fourth body	Unit
	τ_3	τ_4	
T_0	2,448,174.52786(19)		HJD
P	0.280419354(10)		d
$a_{12} \sin i_{3,4}$	2.342(41)	0.418(55)	AU
ω	166.8(1.7)	139.7(7.5)	deg
e	0.488(27)	0.723(104)	
n	0.017874(76)	0.06206(19)	deg d ⁻¹
T	2,428,381(89)	2,423,967(83)	HJD
$P_{3,4}$	55.15(23)	15.88(5)	yr
K	0.01190(21)	0.00201(26)	d
$f(M_{3,4})$	0.004227(76)	0.000289(38)	M_\odot
$M_{3,4} \sin i_{3,4}$	0.223(2)	0.107(5)	M_\odot
A	$-3.778(46) \times 10^{-11}$		d
dP/dt	$-9.84(12) \times 10^{-8}$		d yr ⁻¹

Table 7. Applegate parameters for the 12-yr period modulation of BX Peg.

Parameter	Primary	Secondary	Unit
ΔP	0.0410	0.0410	s
$\Delta P/P$	1.69×10^{-6}	1.69×10^{-6}	
ΔQ	2.81×10^{48}	7.54×10^{48}	g cm ²
ΔJ	2.01×10^{46}	3.89×10^{46}	g cm ² s ⁻¹
I_s	9.48×10^{52}	6.11×10^{53}	g cm ²
$\Delta \Omega$	2.12×10^{-7}	6.35×10^{-8}	s ⁻¹
$\Delta \Omega/\Omega$	8.18×10^{-4}	2.45×10^{-4}	
ΔE	8.53×10^{39}	4.94×10^{39}	erg
ΔL_{rms}	6.96×10^{31}	4.03×10^{31}	erg s ⁻¹
	0.018	0.010	L_\odot
	0.055	0.016	$L_{\text{p,s}}$
Δm_{rms}	± 0.020	± 0.011	mag
B	11.2	8.1	kG

Table 8. Light levels of BX Peg at four different phases.

Mean Year	Mean Epoch	Min I		Max I		Min II		Max II		Ref.
		ΔV	ΔB	ΔV	ΔB	ΔV	ΔB	ΔV	ΔB	
1978.84	-15537.50	0.637	0.348	0.009	-0.309	0.612	0.330	0.011	-0.320	1
1988.63	-2787.62	0.736	0.406	0.127	-0.251	0.709	0.367	0.104	-0.278	2
1999.83	11807.24	0.785	0.498	0.157	-0.160	0.749	0.455	0.125	-0.198	3
2000.67	12897.27	0.776	0.486	0.133	-0.197	0.700	0.410	0.112	-0.191	3
2008.81	23490.45	0.890	0.622	0.226	-0.076	0.765	0.495	0.207	-0.094	4
		0.765	0.472	0.130	-0.199	0.707	0.411	0.112	-0.216	5

References. — (1) Zhai & Zhang (1979); (2) Samec (1990); (3) Lee04a; (4) this article; (5) mean value.